Scientific Research Publishing

Journal of High Energy Physics, Gravitation and Cosmology, 2022, 8, 285-302
https://www.scirp.org/journal/jhepgc
ISSN Online: 2380-4335
ISSN Print: 2380-4327

Higher Order Self-Induced Self-Interacting Field

Edwin Eugene Klingman

Cybernetic Micro Systems, Inc., San Gregorio, CA, USA
Email: klingman@geneman.com

How to cite this paper: Klingman, E.E. (2022) Higher Order Self-Induced Self-Interacting Field. *Journal of High Energy Physics, Gravitation and Cosmology*, **8**, 285-302.
https://doi.org/10.4236/jhepgc.2022.82023

Received: January 5, 2022
Accepted: March 27, 2022
Published: March 30, 2022

Abstract

The genesis of physical particles is essentially a mystery. Quantum field theory creation operators provide an abstract mechanism by which particles come into existence, but quantum fields do not possess energy density. I reference several recent treatments of this problem and develop ideas based on self-stabilizing field structures with focus on higher order self-induced self-stabilizing field structures. I extend this treatment in this paper to related issues of topological charge.

Keywords

Self-Stabilized Field Theory, Self-Organizing Structure, Topological Charge, First-Order Dynamics, The Biot-Savart Law, Ampere's Law, Neutrino, Heaviside Equations, Gravitational Field, Solitons, Self-Dual, Self-Aware, Gauss-Linking

1. Introduction

Heaviside equations are scale-independent except for a tension term $\left(\frac{c^2}{g}\right)=\frac{m}{l}$ mass/unit length

$$\left(\frac{m}{l}\right)\nabla\times\boldsymbol{C}=-\rho_m\boldsymbol{v}+\frac{\mathrm{d}}{\mathrm{d}t}\left(\frac{\boldsymbol{G}}{g}\right) \tag{1}$$

tension·circulation = momentum density

where $\boldsymbol{C}$ is the gravitomagnetic field, $\boldsymbol{G}$ is the Newtonian gravitation field, and ρ_m is the mass density moving with velocity $\boldsymbol{v}$ that induces the gravitomagnetic field circulation. Density is scale dependent; hence the induced circulation is scale dependent. For example, *Gravity Probe B* [1] measured the C-field induced by the Earth's rotation, based on the density of Earth. If we compare this to the circulation induced by an electron, we expect significantly higher circulation locally. This fact has been overlooked for a century. We grow up with Newtonian gravity based on mass and even our best experts tend to retain this perspective: "*To get a meaningful amount of gravity, you need a large amount of mass.*" [2] If one restricts *gravity* to Newtonian gravity, this is true, but that leaves some of the most fascinating areas of Heaviside gravity theory, those aspects covered by Equation (1), completely unrecognized. Additionally, general relativity texts almost unanimously treat the Heaviside equations as the weak field approximation to Einstein's nonlinear equations, the error of which has only recently been recognized. This opens new areas of relevance to gravity; we review the concepts necessary to pursue these new areas. Our goal is to develop a theory of particle genesis based on the primordial gravitational field, but to do so requires several concepts typically missing from general relativity texts. The plan of this work is as follows:

Section 2 reviews the concept of physical energy density versus the geometric abstraction of relativity. In particular, the most relevant energy densities lend themselves to the concept of super fluid, which is introduced here.

Section 3 introduces the concept of quasiparticles. Although our goal is the genesis of real particles from gravity, it becomes easier to cross correlate gravitational concepts and particle physics concepts via this intermediate step.

Section 4 emphasizes the connection between energy density of fields and scale independence.

Section 5 introduces the concept of topological linking, relating it to previous papers by the author and also to recent interesting work in other fields, including photonics.

Section 6 introduces the self-dual nature of C-field structure in terms of analogy with electromagnetic structures treated in the previous section.

Section 7 presents stability ideas built on familiar concepts of solenoidal-like structures.

Section 8 discusses the dynamical evolution from vortex structure to toroidal structure, both of which are fundamental to particle evolution from ultra-dense gravitational fields.

Section 9 builds on the previous concepts to develop a representation of higher-order self-interaction, the fundamental process whose stability we analyze herein.

Section 10 begins the dynamical analysis of higher-order self-interacting structure.

Section 11 presents the summary and conclusions of this paper.

2. Physical Energy Density vs Geometric Abstraction

Most relativity is mass-based, even though field theories are density-based and the belief that "real gravity" is nonlinear curved space-time and that Heaviside's equations are the *weak field approximation* to gravity obtained by throwing away non-linear terms. *The Primordial Principle of Self-Interaction* [3] derives Heaviside's equations from $\nabla\psi = \psi\psi$ using Hestenes' geometric calculus. The most significant aspect of this derivation is that the concept of field strength appears nowhere in it, other than the supposition that the self-interaction equation describes the primordial field, assumed created at the big bang. That is, the equations are assumed to hold for strong field (ultra-dense) physics as well as the weak field approximation to Einstein's equation.

There is still belief that curved space-time is the "true" theory of gravity, despite that physicists from Feynman to Deser have shown that Heaviside equations, iterated properly, are exactly equivalent Einstein's non-linear formulation. Although Feynman, Weinberg, Padmanabhan and others have insisted that "curved space-time" is not a necessary concept for gravity, many do not take this seriously. The paper *Encoding Energy Density as Geometry* [4] analyzes the never-solved problem of gravitational energy in general relativity and defines the procedure that produces the metric from energy density distributed over Euclidian space. Given this equivalence of Heaviside's equations to Einstein's geometric formulation, one would expect no differences in the results obtained. However, Almeida remarks [5]:

> "The choice of a particular algebra is irrelevant from the point of view of the mathematical validity of the equation, but it may make a significant difference to the perception and comprehension of the physics behind the equations."

Therefore, in the remainder of this paper we assume that the Heaviside equations are (iteratively) equivalent to Einstein's nonlinear equations and apply at *all* field strengths, including those found in ultra-dense fields, and by ultra-dense is meant those densities found at the big bang and potentially found in collisions of heavy atomic nuclei with each other at the Large Hadron Collider. Circa 2006 experimenters expected collisions to produce a *quark gas*; they found a *perfect fluid*. This is compatible with cosmological perfect fluid models such as formulated by Huang in "*A Superfluid Universe*" [6] or Volovik in "*The Universe in a Helium Droplet*" [7]. The C-field detected by *Gravity Probe B* is weak and relevant densities are low; a C-field occurring when particles smash into each other and effectively dissolve into a locally turbulent perfect fluid is ultra-dense and the local field strength potentially capable of exerting relevant force. Per Dyson [8] Maxwell was extremely impressed with Helmholtz's proof that

> "…in the perfect fluid, a whirling ring, if once generated, would go on whirling forever."

Dyson almost scoffs at Maxwell's appreciation of Helmholtz's support for Thompson's vortex model of atoms. Of course, Maxwell did not distinguish atoms from fermions because Maxwell did not know of fermions; but Dyson did.

3. Quasi-Particles: Local vs. Topological

General relativity solves static one-body problems in *curved space* metrics such as Schwarzschild and Kerr. By encoding energy density as geometry, we derive the Schwarzschild metric $g_{00} = 1 - 2\phi$ via an energy normalization procedure defining the *curved space* equivalent of flat space energy distribution. The extended Kasner metric, $K^N V$, is a dynamic metric best interpreted through the gravitomagnetic field interpretation, as done in *A Primordial Space-Time Metric* [9]. The $K^N V$ approach assumes with Einstein that "*there is no space absent a field*"; the *field* is physically real—the *space* is an abstraction of the human mind. The metric, expressed in C-field terms leads to C-field dynamics governed by Heaviside; as seen in **Figure 1**, with apparent density variations as might be generated when gravito magnetic field lines reconnect. The Kasner metric describes an *empty* universe, empty of matter, but our insistence on a perfect fluid primordial field assumes that turbulence produces density variations, and the consequent ultra-dense disturbances in the field propagate through the field. Roychaudhuri has pointed out that the Huygens model *propagates forever* [10] and he emphasizes the primary parameters ε_0^{-1} and μ_0 instead of secondary parameter $c = \sqrt{\varepsilon_0^{-1}/\mu_0}$. This is compatible with Lightman and Lee's $TH\varepsilon\mu$ model, described by Will as capable of hosting all theories of gravity in a frame in which non-gravitation electromagnetic entities exist [11]. All the above reinforces the conclusion that Heaviside equations are more suitable than Einstein's equations for understanding dynamic gravity. We retain Einstein for certain connections, such as Calabi-Yau manifolds; for most problem-solving work we employ Heaviside, augmented [12] by the inverse operator $(\nabla\times)^{-1} = (\boldsymbol{r}\times)$.

Since we ultimately intend to derive particles from the primordial gravitational field, we temporarily switch the focus from General Relativity to the current particle physics formulation. In *Lattice Gauge Theory*, DiGiacomo remarks [13] that Euclidean QCD admits classical solutions with finite action and with non-trivial topology which makes them stable and labels these solutions instantons. The approach is quite general. In this work and its follow-on efforts, we consider the $S^2 \times S^2$ instanton as the key topological manifold underlying physical particles. The generality of this approach is illustrated by Volkov and Wipf's [14] derivation of the spectra of small fluctuations around $S^2 \times S^2$ instantons in a basis that splits the ten coupled gravity fluctuation equations into ten independent equations, such that an exact one-loop calculation of the tunneling process in Euclidean describes creation of a black hole pair in an isotropic deSitter universe.

This exact one-loop calculation of creation of a black hole pair in an isotropic deSitter universe is in tune with the recent remark [15]: *"General relativity is a highly successful theory which has been used to model the universe on many different scales. On the 'microscopic' scale of individual stars and stellar black holes, it has been tested and confirms with great accuracy…"*

In *Primordial Space-time Metric* I derive scale invariant pair creation in a dynamic, anisotropic universe with translation symmetry in which the ground state has uniform energy density. I introduce an excitation and observe the energy density over the space. In a local region the energy density is higher than the ground state, thus there is a *particle-like* excitation, or quasiparticle locally. If

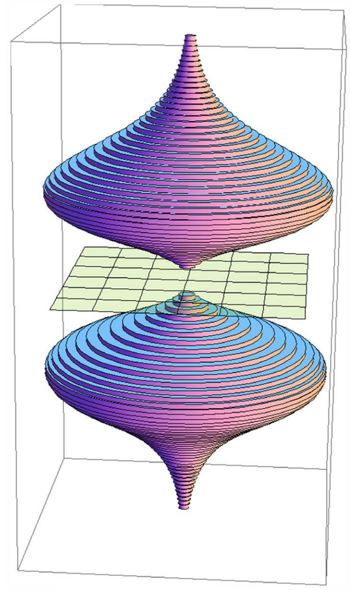

Figure 1. Topological quasi-particles in Kasner space excited by a gravitomagnetic field reconnection event.

such a particle can be created or annihilated by local operators, such as spin flip, then they are not robust under perturbations, and are labeled local quasiparticles. A robust, or stable state that cannot be created or removed by any local operator, is a topological quasiparticle. The excitation in $K^N V$-metric, shown in **Figure 1**, is such a topological quasiparticle, excited by a (nonlocal) gravitomagnetic reconnection event.

In anticipation of future results of this theory we introduce terminology that is only incidental to this paper. Specifically, a topological quasiparticle *type* is a *topological charge*. Local quasiparticles are said to be trivial, while topological charge is nontrivial. In fact, the total number of topological quasiparticles is also a topological property, since topological charges are of the same type if and only if they differ by local quasiparticles. For topological states the number of topological charges is equal to the ground state degeneracy on $S^2 \times S^2$; the torus.

4. Energy Density—Scale Invariance

The goal of describing the *scale* and *shape* of space is to encompass *all* scales of space. For example, propagating energy densities shown in **Figure 1** are scale undetermined. Values of energy-density, distance, and time are scaled to yield convenient numbers for dynamic presentation. To do so we must be able to show that $\nabla \psi = \psi \psi$ is scale independent. The field determined by solving the primordial self-interaction equation, $\nabla \psi = \psi \psi$, is $\boldsymbol{\psi} = \mathbf{r}/r^2$.

If we rescale $\boldsymbol{r}$ via $\boldsymbol{r} \rightarrow \lambda \boldsymbol{r}$ then

$$\boldsymbol{\psi}(\lambda \boldsymbol{r}) = \lambda \mathbf{r}/\lambda^2 r^2 = \lambda^{-1} \mathbf{r}/r^2 = \lambda^{-1} \boldsymbol{\psi}(\boldsymbol{r}). \tag{2}$$

Since

$$\boldsymbol{r} \rightarrow \lambda \boldsymbol{r} \Rightarrow \boldsymbol{\psi}(\boldsymbol{r}) = \lambda \boldsymbol{\psi}(\lambda \boldsymbol{r}) \tag{3}$$

the solution field configuration is scale invariant according to the (Wikipedia?) requirement that

$$\psi(x) = \lambda^{-\Delta}\psi(\lambda x). \quad (4)$$

We next show that the primordial self-interaction equation, $\nabla\psi = \psi\psi$, is scale invariant by replacing the original field $\psi(\mathbf{r})$ with rescaled field $\lambda\psi(\lambda\mathbf{r})$ in equation $\nabla\psi(\mathbf{r}) = \psi(\mathbf{r})\psi(\mathbf{r})$.

$$\nabla(\lambda\psi(\lambda\mathbf{r})) = \lambda\psi(\lambda\mathbf{r})\lambda\psi(\lambda\mathbf{r}) \Rightarrow \nabla\psi(\lambda\mathbf{r}) = \lambda\psi(\lambda\mathbf{r})\psi(\lambda\mathbf{r}) \quad (5)$$

$$\nabla\left(\frac{\mathbf{r}}{\lambda r^2}\right) = \lambda\lambda^{-1}\psi(\mathbf{r})\lambda^{-1}\psi(\mathbf{r}) \Rightarrow \frac{1}{\lambda}\nabla\psi(\mathbf{r}) = \frac{1}{\lambda}\psi(\mathbf{r})\psi(\mathbf{r}) \quad (6)$$

hence the Heaviside-Hertz equations are scale independent, so we seek to find *any* stable solution. If such a solution exists, it is assumed that the structure becomes *real* for *one* scale and corresponding density of all possible scales and densities, *i.e.*, the energy profiles shown in **Figure 1** are realistic for *some* scale and local density in the gravitation-based $K^N V$ -metric.

Thus, our goal is to find and construct stable field structures, which we identify as material particles. Importance of this construction is hinted at by the Millennium $1 million prize for solving the *Mass Gap* problem. The field is a continuum; it would seem that all field-based masses, down to zero, would occur. The fact that fermions have a mass gap between their mass and the (massless) ground state cannot yet be shown via rigorous Yang-Mills-based proof, or even explained. Stable field structures can explain the *mass gap*.

Our conjecture is that any field-based construct representing the particle must be self-stable—the field must hold itself together for indefinite periods of time. This demands an emphasis on stability and building a stable structure from a dynamic field. How do we determine shape of the structure?

5. Topological Linking

Topological states probably first entered physics in the analysis of energy bands in condensed matter physics. In crystals, two bands may cross each other and form degeneracies along a closed loop in three-dimensional momentum space, which is called a nodal line. Nodal line degeneracy can be designed to exhibit various configurations such as nodal rings, chains, links, and knots.

Yang *et al.* [16] experimentally demonstrated non-Abelian nodal links in an explicitly designed microwave metamaterial, producing the nodal links shown in **Figure 2(a)**. The design consists of an array of thin metallic wires and metallic cross structures patterned on a dielectric plate. The cross structures with arms along the $x = \pm y$ directions provide the anisotropy in the x and y directions. The bulk modes propagating in the metamaterial are simulated via commercially available software—*CST Microwave Studio*.

The linkages created by explicit design using metamaterials illustrate the type of non-Abelian nodal links observable in photonics, which are expected to be much richer than topologies associated with the evolution of self-interacting

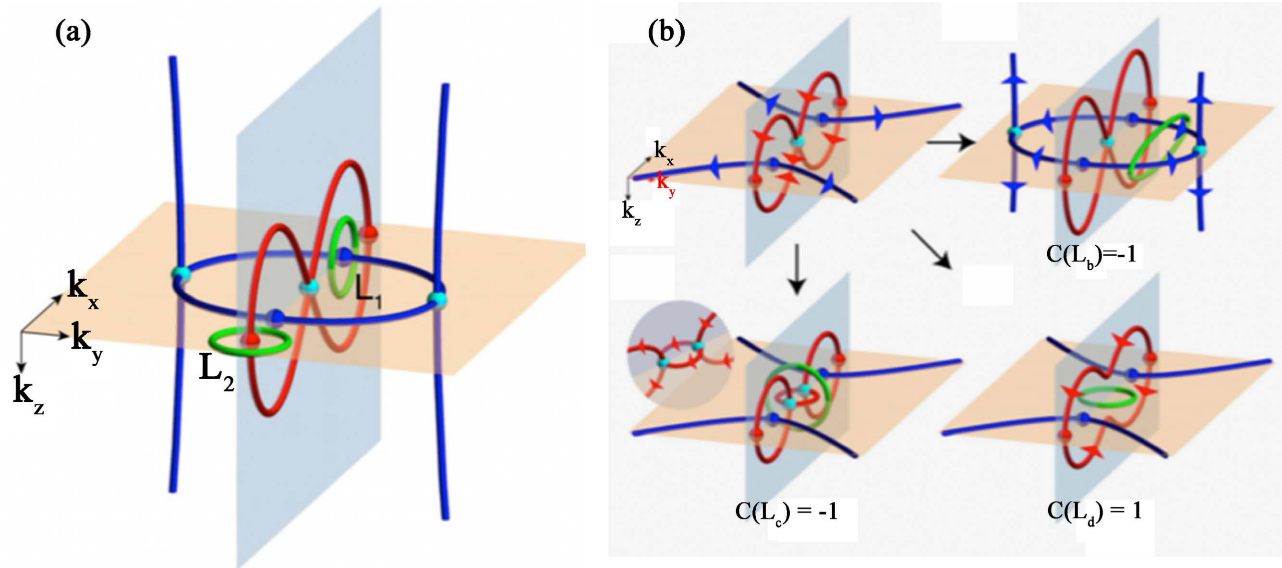

Figure 2. Examples of nodal linking in meta-materials used in photonics *Phys Rev Lett* **125**, 033901 (2020).

gravitomagnetic field structure, which is our focus in this work.

A Self-linking Field Formalism [17] shows that the electromagnetic field supports Gauss-linking, but is *not* self-linking and hence not capable of forming stable final configurations. Based on work of DeTurck and Gluck [18], I defined a self-dual, self-linking field and showed that the gravitomagnetic field of Heaviside's Equation (1) *is* self-dual and self-linking and that first-order induced fields inherently induce second and higher order induced fields; the higher order induced fields reinforce the primary source of induction.

After finding the electromagnetic geon to be inherently unstable, Wheeler then imagined a "purer" geon—*one made up of gravitational energy alone*—and hoped that quantum effects might make possible a geon as small as a particle: "*mass without mass*", but he never succeeded in this quest. That is the quest we take up here; to construct a particle made up of gravitational energy alone.

We are not alone in this quest. Recently [19] Alexander Burinskii sought to unify gravity with particle physics based on the Kerr-Newman metric solution to Einstein's field equations. However a KN ring singularity branches Kerr space into two sheets and this two sheetedness represents one of the main puzzles of the KN space-time; it is not *a priori* clear that a valid model can be realized. Most interesting is Burinskii's analysis identifying "*weakness of gravity as an illusion… the question of consistency with gravity is not discussed usually for solitonic models, as it is conventionally assumed that gravity is weak and not essential at scale of electroweak interactions.*" He claims that assumption of weakness of gravity is "*an illusion, related to underestimation of the role of spin in gravity.*" The spin of elementary particles is extremely high; in dimensionless units $(G = c = \hbar = 1)$ the electron spin/mass ratio is about 10^{22}. He concludes: "*similar to cosmology where giant masses turn gravity into a main force", the giant spin of particles makes gravity strong!* This observation is relevant to the fact that the essence of gravito magnetism is angular momentum density.

We view stable constructions in electromagnetic field theory as models we should study in detail. With a helical current we can induce an axial field and with an axial source we can induce a helical field. These structures consist of two physical entities, field, and charge.

6. The Self-Dual Structure of the C-Field

The gravitomagnetic field is unique: the field energy density of the circulating field has momentum density $\boldsymbol{C}\cdot\boldsymbol{C}\cong|\boldsymbol{p}|$. This marvelous property follows from $E=mc^2$; energy has *mass equivalence*. This is not a static relation; it is dynamic in the case of the C-field. Einstein and deHaas [20] proved that the magnetic field *possesses* angular momentum; the gravitomagnetic field *is proportional to* angular momentum. That is, the C-field incorporates motion and the energy density of the field in motion instantiates momentum density $\boldsymbol{p}$. Therefore, unlike the electromagnetic structures of **Figure 3**, which require (uncharged) magnetic field plus charge density, the gravitomagnetic field provides its own momentum density, and is thus potentially self-stable, as depicted in **Figure 4**.

The structure shown in **Figure 4** is not yet guaranteed to be stable, but at least the self-interactive property of the gravitomagnetic field suggests that such a structure might exist. Recall that Wheeler's *geon*, or "self-captured light structure", was based on the self-gravity of the light energy and required cosmological scale; even this was not stable. We thus wish to analyze two aspects of the C-field—*scale* and *stability*.

7. Stability Issues in Solenoidal-Like Structures

Physicists and electrical engineers have sufficient experience building electromagnetic solenoids that most develop an intuitive feel for such. Therefore, we

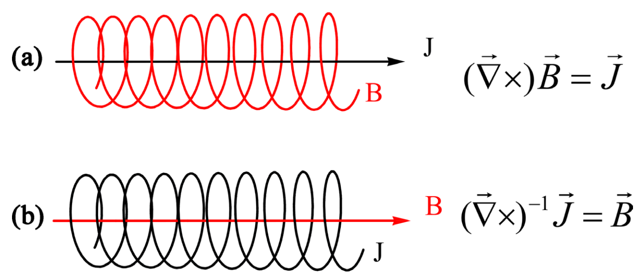

Figure 3. (a) Linear charge current density $\boldsymbol{J}$ induces magnetic $\boldsymbol{B}$ field circulation; (b) Solenoidal current induces axial magnetic field $\boldsymbol{B}$.

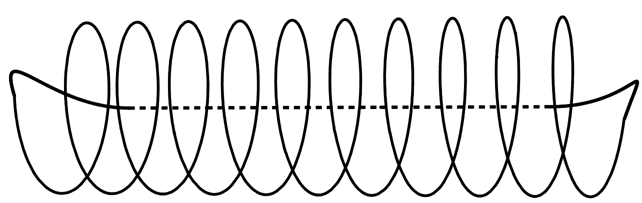

Figure 4. Self-dual, self-linked solenoidal structure of the gravitomagnetic field.

consider electromagnetic structures before moving to consider analogous gravitomagnetic structures. Of particular interest is the energy analysis of "open" and "closed" helical structures, as depicted in **Figure 5**.

Examine the magnetic field induced by a helical current flow. Assume that half of the induced field is concentrated on the axis of the helix while the other half is distributed over space outside the helix. If the helix is bent into a torus, *all* of the magnetic field is confined to the axis; thus the closed structure has higher energy density and is considered more stable from several aspects. By constraining helical current flow to metallic wires, we can build the above structures and experiment with the physical dynamics. But this assumes an *agent* designing and shaping structures; significantly different from the issue of evolving self-stabilized structures from the primordial field. That helical structures evolve in the primordial field is strongly implied by the fact that vortical structures occur naturally and evolve.

For instance, my grandson last week remarked that the vortices induced in water by the tip of the oar maintained the structure of the vortex for an extended period. Moreover, Chen, *et al.* [21] report observations of discrete vortex bound states with energy levels deviating from widely believed ratio of 1:3:5 in the vortices of an iron-based superconductor $KCa_2Fe_4As_4F_2$ via scanning tunneling microscopy (STM). In addition, Friedel oscillations of vortex bound states are also observed for the first time in related vortices. "*For a vortex in a type-II superconductor, it is generally understood that the quantized magnetic flux of* $\Phi = h/2e = 2.07 \times 10^{-15}$ Wb *distributes in the region with the radius of penetration depth* λ."

Vortex bound states can appear in clean superconductors based on the solution to the Bogoliubov-deGennes (BdG) equations. Chen *et al.* also observe energy ratios deviating from the expected 1:3:5, and Friedel oscillations surrounding vortex center of energies which cannot be explained by the theory. We do not concern ourselves with the specific very special vortices, but only that stable vortices exhibit dynamics with unexplained energy distributions.

8. Vortex Dynamics: Evolution from Vortex to Torus

From watching tornados, we know that vortices can lengthen indefinitely until

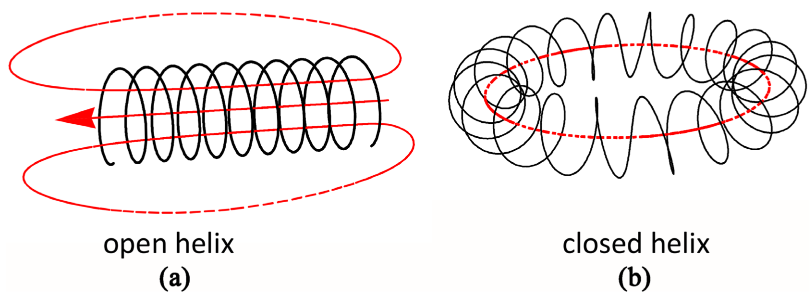

Figure 5. (a) The field induced by helical current in an open helix resides both on the helical axis and is distributed over space surrounding the helix; (b) Magnetic field induced by the same current in a closed helix is constrained to reside on the (closed) helical axis; total induced field is assumed to be the same, thus the closed-helix-induced energy-density is assumed greater than the axial density of the open helix.

they reach the ground. The environment of the Big Bang is anything but calm. One can imagine neighboring vortices colliding, or even a vortex within another larger vortex. In any event we can expect a long vortical tube to bend in sufficient turbulence, as depicted in Figure 6.

How stable is such a vortex? In Figure 4 induced circulation $\boldsymbol{C}'$ is generated by momentum density of axial flow $(\boldsymbol{C}\cdot\boldsymbol{C})\boldsymbol{v}$ while the $\boldsymbol{C}$ circulation is enhanced by the $\boldsymbol{C}'$ circulation around the axis. As the head of the vortex collapses around the swallowed tail, it generates a Lenz-law-like "gmf" (gravito-motive-force). The circulation $\nabla\times\boldsymbol{C}$ is proportional to momentum-density $\boldsymbol{p}$, that is

$$\nabla\times\boldsymbol{C}\sim\boldsymbol{p} \tag{7}$$

hence

$$\frac{\mathrm{d}}{\mathrm{d}t}(\nabla\times\boldsymbol{C})\sim-\frac{\mathrm{d}\boldsymbol{p}}{\mathrm{d}t} \tag{8}$$

where $\mathrm{d}\boldsymbol{p}/\mathrm{d}t$ is the force density corresponding to the change in circulation with time. If there is no change in the circulation, there will be no change in the momentum. This gmf provides Feynman's missing explanation for the conservation of momentum. The system in a perfect fluid is *not* lossy. The field lines farthest from the axis of the helix have the least support for existing, and their collapse induces a gravitomagnetic pulse reinforcing the local momentum of the field.

Having developed a *vortex-helix-torus* model that, based on observation of physical reality, is ubiquitous, let us close the open helix into a torus and examine this in terms of gravity. Recall that Einstein and deHaas experimentally proved that the electromagnetic field has angular momentum. The gravitomagnetic field is directly proportional to angular momentum density:

$$\boldsymbol{C}\sim(\nabla\times)^{-1}\,\boldsymbol{p}=\boldsymbol{r}\times\boldsymbol{p} \tag{9}$$

9. Higher-Order Self-Interaction

The circulating field flows in the perfect fluid—the fact that so fascinated

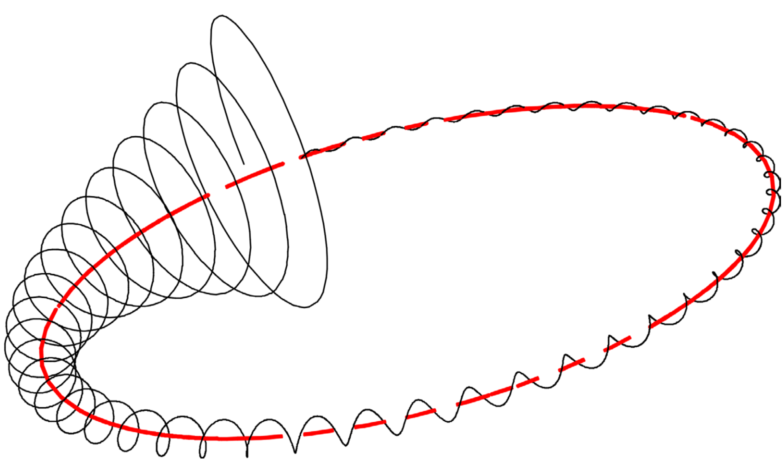

Figure 6. One possible evolution of a self-sustaining vortex field structure.

Maxwell—the local field is flowing, under its own influence, in an endless loop. This flow is along the 2D surface of the 4D doughnut in space-time. Such a flow is impossible for spheres, which have two points of discontinuity on the sphere: the poles, where the "wind" cannot flow in any direction. There is no point on the surface of the torus that frustrates flow. This is known as the vanishing Chern class of Hermitian manifolds and is a key topological property.

The diagram of **Figure 7** illustrates first and second order induced fields caused by source momentum density, p_0. We can carry this scheme further as shown in **Figure 8**, which shows theoretical high order inductions of C-field circulations and illustrates the nature of successive higher order interactions. It may be useful in the same way that a Taylor series is useful, to help draw conclusions.

The first conclusion is that successive orders do *not* interact to any degree; they are orthogonal, hence the force $\boldsymbol{p} \times \boldsymbol{C}$ is always zero. Alternate orders, on the other hand, *do* interact, as they are parallel or anti-parallel. To schematically illustrate this we take the tangent vectors to the circulation loops at the nearest and farthest points and "square the circle", using the straight lines as heuristic devices to facilitate the expression of forces involved via analogy with electromagnetic forces between parallel currents. The self-linking field formalism of **Figure 7** shows that second-order induction reinforces the primary inducing agent, *i.e.*, local momentum density $\rho \boldsymbol{v}$. Following Duckworth's description of the electromagnetic force $\boldsymbol{F}_{ij}$ between two current elements $\mathrm{d}\boldsymbol{j}_i$ and $\mathrm{d}\boldsymbol{j}_j$ a distance $\boldsymbol{r}_{ij}$ apart we write the gravitomagnetic equivalent

$$\mathrm{d}\boldsymbol{F}_{ij} = \frac{\left[\mathrm{d}\boldsymbol{p}_j\right] \times \left[\mathrm{d}\boldsymbol{p}_i \times \boldsymbol{r}_{ij}\right]}{r_{ij}^3}. \tag{10}$$

Since $\mathrm{d}\boldsymbol{C}_i = \mathrm{d}\boldsymbol{p}_i \times \frac{\boldsymbol{r}_{ij}}{r_{ij}^3}$ where $\mathrm{d}\boldsymbol{p}_i$ is the mass current element inducing the

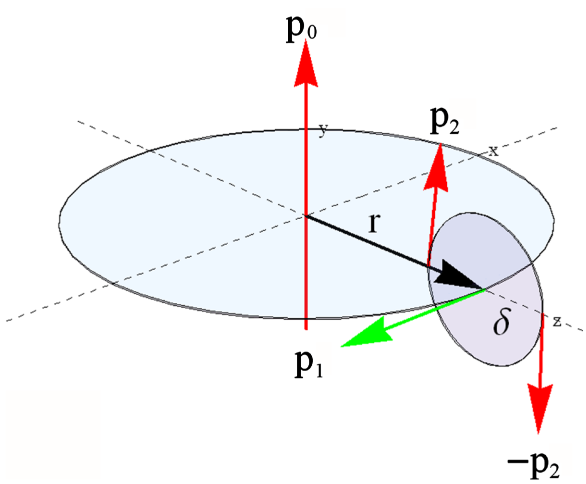

Figure 7. Momentum density $\boldsymbol{p}_0$ (red) induces C-field circulation at position $\boldsymbol{r}$. The C-field circulation at $\boldsymbol{r}$ yields momentum density $\boldsymbol{p}_1$ (green) orthogonal to $\boldsymbol{p}_0$. Momentum $\boldsymbol{p}_1$ induces the C-field at distance δ from $\boldsymbol{p}_1$. This induced C-field yields momentum density $\boldsymbol{p}_2$ (red) with components parallel and anti-parallel to $\boldsymbol{p}_0$.

field then $\mathrm{d}\boldsymbol{p}_j \times \mathrm{d}\boldsymbol{C}_i$ and Equation (10) is seen to be compatible with the Lorentz force law $\boldsymbol{F} = \boldsymbol{p} \times \boldsymbol{C}$ for the force on momentum $\boldsymbol{p}$ in gravitomagnetic field $\boldsymbol{C}$. In *A Self-linking Field Formalism* I show first-order C-field induction from momentum source density $\boldsymbol{p}_0$, and then derive the second order C-field induction from the momentum of the first-order field, $\boldsymbol{p}_1 \sim \boldsymbol{C}_1 \cdot \boldsymbol{C}_1$. as shown in Figure 7.

The nature of the *C*-field symmetry implied by Heaviside's equations, $\nabla \times \boldsymbol{C} \sim \boldsymbol{p}$, is *U*(1) since $\boldsymbol{C} \sim \boldsymbol{C}\mathrm{e}^{-i|C|t}$. In *Superfluid States of Matter* [22] it is noted that to demonstrate the phenomenon of superfluidity, the linear model

$$i\frac{\partial \psi}{\partial t} = -\frac{\gamma}{2}\nabla^2 \psi \tag{11}$$

must be generalized to become nonlinear (*i.e.*, self-interactive) while *U*(1) symmetry is preserved. The simplest self-interaction consistent with *U*(1) invariance of the Hamiltonian is introduced by the $|\psi|^4$ term.

$$H \to H + \left(\frac{g}{2}\right)\int |\psi|^4 \, \mathrm{d}^d r \tag{12}$$

with positive interaction constant *g*. For constant gravity $\dot{G}/g$ the field $\boldsymbol{\psi}(\boldsymbol{r}) \to \boldsymbol{C}(\boldsymbol{r},t) \sim \rho_m$ for $c = 1$. Thus, the first order self-interaction yields the local energy density associated with the zeroth order source momentum density (the topological charge of the vortex). We have seen that the orthogonality of the induced field implies that $\psi\psi\psi' \equiv 0$, while $\psi\psi\psi'\psi' \neq 0$, hence $|\psi|^4$ is the first relevant higher order self-interaction consistent with the above.

The local environment is best represented by an inhomogeneous external potential $\mathcal{V}(\boldsymbol{r})$, hence

$$H \to H + \int \mathcal{V}(\boldsymbol{r}) |\psi(\boldsymbol{r})| \mathrm{d}^d r \tag{13}$$

with the new Hamiltonian

$$H = \int \left(\left(\frac{\gamma}{2}\right) |\nabla \psi|^2 + \mathcal{V}(\boldsymbol{r}) |\psi|^2 + \left(\frac{g}{2}\right) |\psi|^2 \right) \mathrm{d}^d r \tag{14}$$

The equation of motion becomes

$$i\dot{\psi} = -\frac{\gamma}{2}\nabla^2 \psi + g|\psi|^2 + \mathcal{V}(\boldsymbol{r})\psi \tag{15}$$

which is the generic nonlinear Schrödinger equation (NLSE) generally known as the Gross-Pitaevski equation, the key equation of superfluidity.

10. Dynamic Analysis of Higher-Order Self-Interaction

Figure 8 shows the idealized structure, in which 5 orders of self-induction are represented. Next consider the way in which we might make use of this representation. In Figure 9 we focus attention on loop1 and loop3 of the structure, showing the source current and second order induction, loop2, as dashed lines. In the figure we note that the bottom current in loop3 is parallel to the rightmost current of loop1, and therefore the currents exert attractive forces upon each

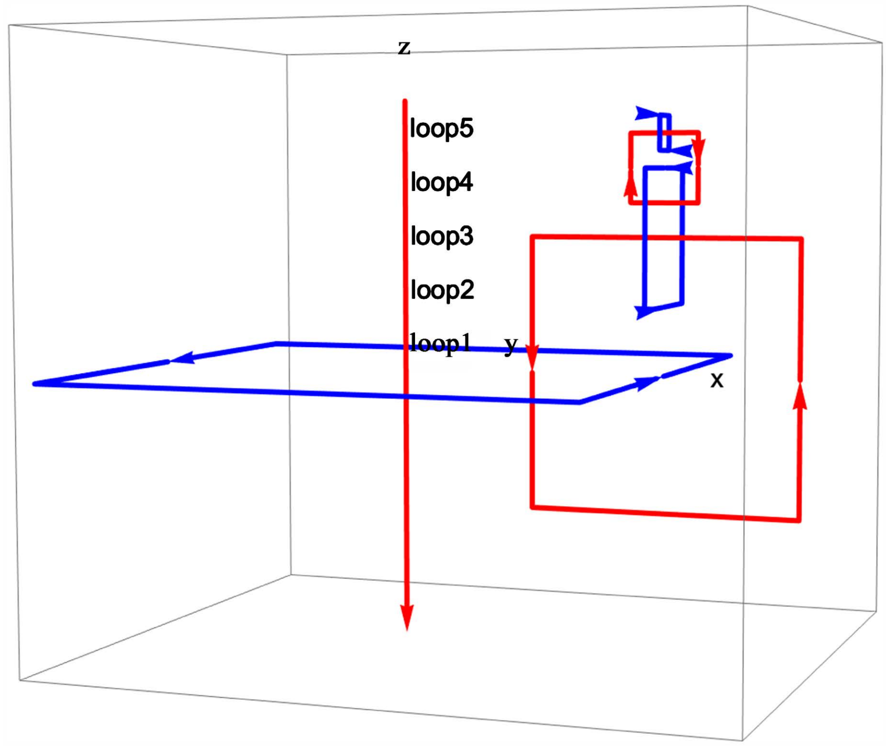

Figure 8. An idealized representation of higher order induction in which every order of induced circulation induces a next order circulation, ad infinitum. The practicality of this concept is dependent on momentum density, $\boldsymbol{p}_0$.

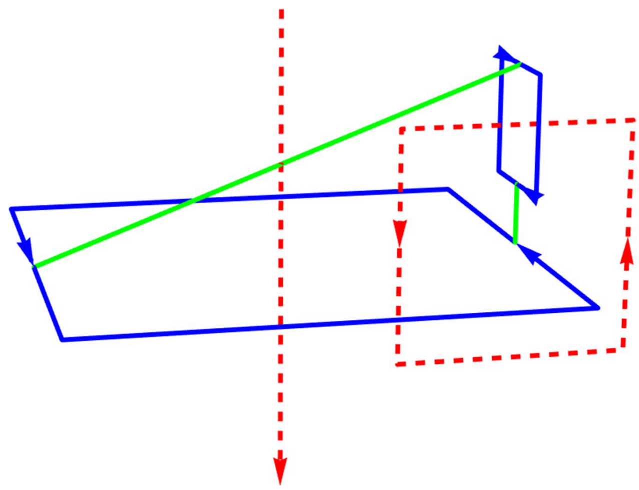

Figure 9. Focusing on loop 1 and loop 3 of the structure shown in **Figure 8**, we downplay source current and second order induction, loop 2, as dashed lines. Since the bottom current in loop 3 is parallel to the rightmost current of loop 1, the currents exert attractive forces upon each other, while top of loop 3 is parallel to the current at the left of loop 1 so the currents attract each other. The attractive force lines are shown in green. The same arguments apply to the anti-parallel currents which exert repulsive forces (not shown).

other. Similarly, the current at the top of loop 3 is parallel to the current at the left of loop 1 and the two currents attract each other. The same arguments apply to the anti-parallel currents which exert repulsive forces. The above follows from

$$\mathrm{d}\boldsymbol{F}_{01} = \mathrm{d}\boldsymbol{p}_1 \times \mathrm{d}\boldsymbol{C}_0 = 0 \text{ since } \boldsymbol{C}_0 \parallel \boldsymbol{p}_1 \tag{16}$$

$$\mathrm{d}\boldsymbol{F}_{02} = \mathrm{d}\boldsymbol{p}_2 \times \mathrm{d}\boldsymbol{C}_0 \neq 0 \text{ since } \boldsymbol{C}_0 \perp \boldsymbol{p}_2 \tag{17}$$

The force between $\boldsymbol{p}_0$ and $\boldsymbol{p}_1$ is zero since these mass density current flows are orthogonal to each other. On the other hand, the force acting between $\boldsymbol{p}_0$ and $\boldsymbol{p}_2$ is maximal when these flows are parallel or anti-parallel.

The representations are exaggerated for heuristic purposes, but nevertheless present a schematic organization to guide calculation of an approximation to the forces involved in the self-interaction of a turbulent primordial field. We seek first a qualitative understanding of dynamic behavior, hopefully followed by a more quantitative approximation. With this goal let us discuss the physics of Figure 9 in the context of Figure 7 and Figure 8.

First, we note that all squares in the diagrams represent extensions of the tangent vectors depicted in Figure 7 so we restore the dashed red loop2 in Figure 8 to its true circular form in the following. With this modification to Figure 9 we expect current loop 3 to rotate about loop 2 as shown, eventually rotating into the xy-plane as depicted in Figure 10.

Several aspects of this idealization must be kept in mind. Loop 3, which we have shown above loop 2, is simply a slice through a torus surrounding loop 2, and has no independent existence such that it can be pulled down into the plane. Nevertheless, if we envision the "slice" pulled into the plane, the field that "replaces" that slice will experience the same forces, so the net result is a dynamic tension that tends to shrink the system of circulations into what we hope to prove is a lower energy configurational state. In another analysis, I believe that the final state of an arbitrary slice can be viewed as a Wilson loop associated with quantum loop gravity, depicted in Figure 11.

Although we have shown schematically the progression to higher order constructions, the behavior is almost certainly governed by interactions between 1st and 3rd order induced circulations, those shown in Figure 9, consisting of the loop1 currents into and out of the page and the two loop 3 circulations, each with parallel currents into and out of the page. To formalize these interactions we define the interaction between momentum density currents p_i and p_j as $g\left[p[i], p[j]\right]$ divided by the absolute distance between the currents, denoted

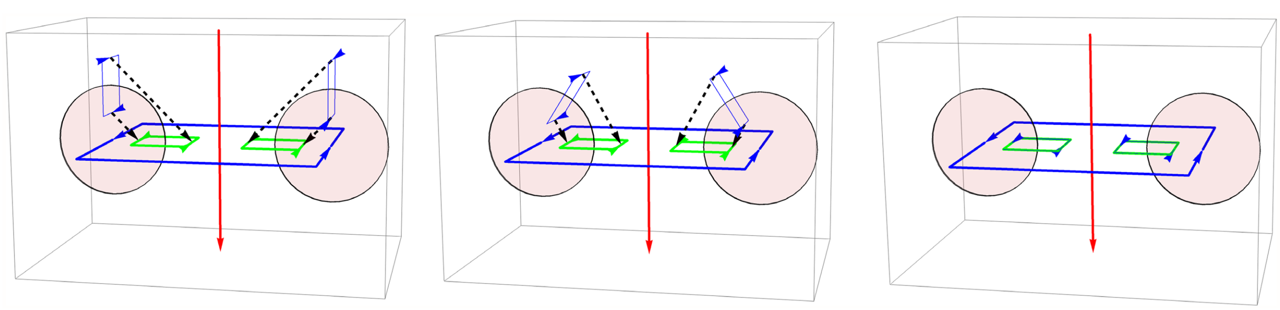

Figure 10. Cartoon snapshots depicting the dynamics of third-order loops interacting with first order loops of induced C-field circulation induced by source momentum $\boldsymbol{p}_0$.

by the term $\text{Abs}\left[p[i]-p[j]\right]$ and construct the interaction matrix over all six relevant currents, as shown in Table 1.

From symmetry arguments the interactions above the diagonal are equal to those below the diagonal, therefore we can reduce the calculations to the form of Table 2.

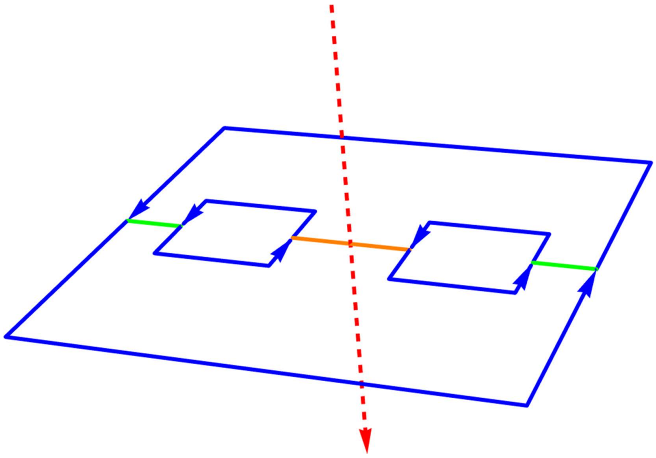

Figure 11. The result of dynamic forces acting on slices of higher order loops are potentially viewed as Wilson loops of quantum loop gravity. In the progression discussed in this paper, the configuration shown exerts attractive forces (green) between the higher order loops and lower order loops and repulsive forces (orange) between the displaced higher order loops. This behavior follows at all orders.

Table 1. Interaction matrix representing the dynamic interactions of Figure 10. Each expression represents an interaction of the type represented by Figure 9.

0	$\frac{g[p[1],p[2]]}{\text{Abs}[p[1]-p[2]]}$	$\frac{g[p[1],p[3]]}{\text{Abs}[p[1]-p[3]]}$	$\frac{g[p[1],p[4]]}{\text{Abs}[p[1]-p[4]]}$	$\frac{g[p[1],p[5]]}{\text{Abs}[p[1]-p[5]]}$	$\frac{g[p[1],p[6]]}{\text{Abs}[p[1]-p[6]]}$
$\frac{g[p[2],p[1]]}{\text{Abs}[-p[1]+p[2]]}$	0	$\frac{g[p[2],p[3]]}{\text{Abs}[p[2]-p[3]]}$	$\frac{g[p[2],p[4]]}{\text{Abs}[p[2]-p[4]]}$	$\frac{g[p[2],p[5]]}{\text{Abs}[p[2]-p[5]]}$	$\frac{g[p[2],p[6]]}{\text{Abs}[p[2]-p[6]]}$
$\frac{g[p[3],p[1]]}{\text{Abs}[-p[1]+p[3]]}$	$\frac{g[p[3],p[2]]}{\text{Abs}[-p[2]+p[3]]}$	0	$\frac{g[p[3],p[4]]}{\text{Abs}[p[3]-p[4]]}$	$\frac{g[p[3],p[5]]}{\text{Abs}[p[3]-p[5]]}$	$\frac{g[p[3],p[6]]}{\text{Abs}[p[3]-p[6]]}$
$\frac{g[p[4],p[1]]}{\text{Abs}[-p[1]+p[4]]}$	$\frac{g[p[4],p[2]]}{\text{Abs}[-p[2]+p[4]]}$	$\frac{g[p[4],p[3]]}{\text{Abs}[-p[3]+p[4]]}$	0	$\frac{g[p[4],p[5]]}{\text{Abs}[p[4]-p[5]]}$	$\frac{g[p[4],p[6]]}{\text{Abs}[p[4]-p[6]]}$
$\frac{g[p[5],p[1]]}{\text{Abs}[-p[1]+p[5]]}$	$\frac{g[p[5],p[2]]}{\text{Abs}[-p[2]+p[5]]}$	$\frac{g[p[5],p[3]]}{\text{Abs}[-p[3]+p[5]]}$	$\frac{g[p[5],p[4]]}{\text{Abs}[-p[4]+p[5]]}$	0	$\frac{g[p[5],p[6]]}{\text{Abs}[p[5]-p[6]]}$
$\frac{g[p[6],p[1]]}{\text{Abs}[-p[1]+p[6]]}$	$\frac{g[p[6],p[2]]}{\text{Abs}[-p[2]+p[6]]}$	$\frac{g[p[6],p[3]]}{\text{Abs}[-p[3]+p[6]]}$	$\frac{g[p[6],p[4]]}{\text{Abs}[-p[4]+p[6]]}$	$\frac{g[p[6],p[5]]}{\text{Abs}[-p[5]+p[6]]}$	0

Table 2. Reduced interaction matrix representing the unique interactions of Figure 10.

0	$\frac{g[p[1],p[2]]}{\text{Abs}[p[1]-p[2]]}$	$\frac{g[p[1],p[3]]}{\text{Abs}[p[1]-p[3]]}$	$\frac{g[p[1],p[4]]}{\text{Abs}[p[1]-p[4]]}$	$\frac{g[p[1],p[5]]}{\text{Abs}[p[1]-p[5]]}$	$\frac{g[p[1],p[6]]}{\text{Abs}[p[1]-p[6]]}$
0	0	$\frac{g[p[2],p[3]]}{\text{Abs}[p[2]-p[3]]}$	$\frac{g[p[2],p[4]]}{\text{Abs}[p[2]-p[4]]}$	$\frac{g[p[2],p[5]]}{\text{Abs}[p[2]-p[5]]}$	$\frac{g[p[2],p[6]]}{\text{Abs}[p[2]-p[6]]}$
0	0	0	$\frac{g[p[3],p[4]]}{\text{Abs}[p[3]-p[4]]}$	$\frac{g[p[3],p[5]]}{\text{Abs}[p[3]-p[5]]}$	$\frac{g[p[3],p[6]]}{\text{Abs}[p[3]-p[6]]}$
0	0	0	0	$\frac{g[p[4],p[5]]}{\text{Abs}[p[4]-p[5]]}$	$\frac{g[p[4],p[6]]}{\text{Abs}[p[4]-p[6]]}$
0	0	0	0	0	$\frac{g[p[5],p[6]]}{\text{Abs}[p[5]-p[6]]}$
0	0	0	0	0	0

In *Superfluid States* we find that as an energy functional H' is minimized for an arbitrary system of fixed shape vortex loops the minimal energy is expressed by the general formula

$$E_{vort} = \frac{\pi}{2}\gamma\rho\sum_{i,j} M_i M_j \int_{|r_i - r_j|} \frac{\mathrm{d}\boldsymbol{l}_i \cdot \mathrm{d}\boldsymbol{l}_j}{|\boldsymbol{r}_i - \boldsymbol{r}_j|} \tag{18}$$

where the (double) line integration is over all the oriented vortex loops, and integer M_i is the winding number of the i^{th} loop, and the direction on the loop is associated with the sense of the circulation of velocity, which is normally set by convention, but in the case of the left-handed C-field is set by Nature. As noted, there are 15 flows of self-interaction, but only six interactions represent dynamic change, in the first approximation, holding loop size constant, hence it is the change in energy associated with these flows that are relevant to stability.

11. Summary and Conclusions

We began by reviewing recent evidence that Heaviside's equations, equivalent to Einstein's geometric equation, are scale independent, hence are density dependent and field strength is a function of density. We demonstrated this point with scale free solutions to the $K^N V$ metric derived from Kasner and Karmarkar-Narlikar. The significance of this is that the gravitomagnetic field, usually erroneously interpreted as the *weak field approximation*, is properly understood as relevant at *all* field strengths, including ultra-dense fields such as those perfect fluids found in LHC nuclear-nuclear collisions and assumed at the big bang.

The self-interactions of the field are distance-based and the distances at the big bang extend at least down to the Planck length. This implies that self-interactions are significant, and the assumption of a primordial field implies that they are the dominant mechanism at work. This theory leads to a focus on stability, and particularly self-stabilized field structures. A previous paper [23] proposed the self-propelling nature of the C-field vortex as a gravity-based soliton model of the neutrino. Here we focus on a "cross-section" of the vortex -> torus.

There are several possible reasons why particle creation has yet to be explained satisfactorily, even though the theory of particle physics successfully *represents* particle creation and annihilation using quantum field theory operators.

First among these is probably the concept of a point particle having a finite extent. This almost demands a spherical structure, which lends itself beautifully to scattering analysis, in terms of which one spherically symmetric point particle scatters another when collisions are close. A mathematically inclined physicist noted that it's impossible to map a sphere into toroidal structure, as if this were relevant. It is relevant only if one assumes that we start with the sphere. The theory of the primordial field starts with a vortex.

The second reason is almost certainly the fact that, for over a century, physicists have believed that Heaviside's equations represent only a weak field approximation to Einstein's nonlinear equations and are non-self-interacting by virtue of higher order terms being intentionally truncated. The recent discovery that post-Newtonian physics applies quite well to extremely strong fields has been met with surprise and is still generally not understood [24]. Associated with this is relativity's focus on mass, despite the density-based nature of field theories.

Still another reason is existence of charge and the incredible strength of electric fields compared to gravitic fields. There are more reasons, but these are generally sufficient to account for the lack, to date, of a theory of gravitational genesis of particles.

The current work is part of a program to derive particles from the primordial field. It began with the derivation of the Heaviside equations from the principle of self-interaction. This derivation is scale free and valid at all field strengths, opening the way to treatment of ultra-dense fields not limited by the *One-body* nature of Einstein's theory. The next major step in the program involved the explanation of physical energy density encoded as geometrical abstraction, which also explains the unsolved problem of local gravitational field energy in general relativity.

Next came focus on the stability of self-interacting field structures, and the proposal that a vortex or gravitational soliton might be viewed as a neutrino, explaining both the minimum mass of the neutrino, conservation of linear momentum, and the neutrino's left-handed chiral nature.

Now we have extended the structure to the $S^2 \times S^2$ or torus and begun the analysis of the higher order self-interactions of the field. We formulated the key terms that should determine the stability of structural change and expect to derive both qualitative and quantitative results in the next step of the program. If, as expected, the stability calculations are positive, there remain two key issues that must be explained, *half integral spin* and *charge*. Some progress has been made on both steps.

Conflicts of Interest

The author declares no conflicts of interest regarding the publication of this paper.

References

[1] Everitt, C.W.V., *et al.* (2011) Gravity Probe B: Final Results of a Space Experiment to Test General Relativity. *Physical Review Letters*, **106**, Article ID: 221101. https://doi.org/10.1103/PhysRevLett.106.221101

[2] Will, C. and Yunes, N. (2020) Is Einstein Still Right? Oxford University Press, Oxford.

[3] Klingman, E. (2020) The Primordial Principle of Self-Interaction. *Journal of Modern Physics*, **12**, 65-81. https://doi.org/10.4236/jmp.2021.122007

[4] Klingman, E. (2021) Encoding Energy Density as Geometry. *Journal of Modern Physics*, **12**, 1190-1209. https://doi.org/10.4236/jmp.2021.129073

[5] Almeida, J. (2009) Different Algebras for One Space-time Reality. In: *Ether*

Space-Time & Cosmology, Vol. 3, Apeiron Pub, Montreal.

[6] Huang, K. (2017) A Superfluid Universe. World Scientific, Singapore. https://doi.org/10.1142/10249

[7] Volovik, G. (2009) The Universe in a Helium Droplet. Oxford University Press, Oxford. https://doi.org/10.1093/acprof:oso/9780199564842.001.0001

[8] Dyson, F. (2007) Why Is Maxwell's Theory So Hard to Understand? 2*nd European Conf. on Antennas and Propagation*, Edinburgh, 11-16 November 2007, 1-6. https://doi.org/10.1049/ic.2007.1146

[9] Klingman, E. (2019) A Primordial Space-Time Metric. *Prespace-Time Journal*, **10**, 671-680.

[10] Roychoudhuri, C. (2012) Space as a Complex Tension Field. *Journal of Modern Physics*, **3**, 1357-1368. https://doi.org/10.4236/jmp.2012.310173

[11] Will, C. (2018) Theory and Experiment in Gravitational Physics. 2nd Edition, Cambridge Press, Cambridge.

[12] Klingman, E. (2020) Exact Inverse Operator on Field Equations. *Journal of Applied Mathematics and Physics*, **8**, 2212-2222. https://doi.org/10.4236/jamp.2020.810166

[13] Di Giacomo, A. (2006) Lattice Gauge Theory. In: Françoise, J.-P., Naber, G.L. and Tsun, T.S., Eds., *Encyclopedia of Mathematical Physics*, Academic Press, Cambridge, MA, 275-281. https://doi.org/10.1016/B0-12-512666-2/00074-2

[14] Volkov, M. and Wipf, A. (2000) Black Hole Pair Creation in deSitter Space. *Nuclear Physics B*, **582**, 313-362. https://doi.org/10.1016/S0550-3213(00)00287-X

[15] te Vrugt, M., Hossenfelder, S. and Wittkowski, R. (2021) A New Approach to the Averaging Problem. *Physical Review Letters*, **127**, Article ID: 231101. https://doi.org/10.1103/PhysRevLett.127.231101

[16] Yang, E., *et al.* (2020) Observation of Non-Abelian Nodal Links in Photonics. *Physical Review Letters*, **125**, Article ID: 033901. https://doi.org/10.1103/PhysRevLett.125.033901

[17] Klingman, E. (2021) A Self-Linking Field Formalism. *Journal of Modern Physics*, **12**, 440-452. https://doi.org/10.4236/jmp.2021.124031

[18] DeTurck, D. and Gluck, H. (2008) Linking, Twisting, Writhing and Helicity on the 2-Sphere and in Hyperbolic 3-Space. *Journal of Differential Geometry*, **94**, 87-128.

[19] Burinskii, A. (2017) Weakness of Gravity as Illusion Which Hides True Path to Unification of Gravity with Particle Physics. *International Journal of Modern Physics D*, **26**, Article ID: 1743022.

[20] Einstein, A. and deHaas, W. (1915) Experimental Proof of Existence of Ampere's Currents. *KNAW Proceedings*, **18**, 696-711.

[21] Chen, X., *et al.* (2021) Friedel Oscillations of Vortex Bound States under Extreme Quantum Limit in $KCa_2Fe_4As_4F_2$. *Physical Review Letters*, **126**, Article ID: 257002. https://doi.org/10.1103/PhysRevLett.126.257002

[22] Svistunov, B., Babaev, E. and Prokof'ev, N. (2015) Superfluid States of Matter. CRC Press, Boca Raton. https://doi.org/10.1201/b18346

[23] Klingman, E. (2021) A Self-Stabilized Field Theory of Neutrinos. *Journal of High Energy Physics, Gravitation and Cosmology*, **7**, 936-948. https://doi.org/10.4236/jhepgc.2021.73054

[24] Will, C. (2011) On the Unreasonable Effectiveness of the Post-Newtonian Approximation in Gravitational Physics. *Proceedings of the National Academy of Sciences of the United States of America*, **108**, 5938-5945. https://doi.org/10.1073/pnas.1103127108